Fabrication of submicron buried metal heterojunction bipolar transistor by EB-lithography

T. Arai, S. Yamagami, Y. Miyamoto, and K. Furuya
Department of Physical Electronics, Tokyo Institute of Technology,
2-12-1 O-okayama, Meguro-ku, Tokyo 152-8552, Japan

A buried metal heterojunction bipolar transistor with submicron emitter was fabricated by electron-beam lithography. Two tungsten wires of 100 nm width, 100 nm height and 200 nm period were buried in the InP collector layer for the device with an emitter area of 0.3×1.5 μm^2. Total base-collector capacitance was reduced to about 22% of that calculated from the physical dimensions of conventional heterojunction bipolar transistors. Current gain cutoff frequency of 82 GHz and maximum oscillation frequency of 200 GHz were obtained.

Introduction

In heterojunction bipolar transistors (HBTs), reduction of the emitter size is effective for operation at low current for power dissipation [1]. In addition, reduction of the emitter size significantly increases the maximum oscillation frequency (f_{MAX}), when extrinsic base-collector capacitance is sufficiently reduced [2].

To reduce base-collector capacitance (C_{BC}), we have proposed the buried metal heterojunction bipolar transistor (BM-HBT) [3]. Tungsten wires were fabricated on semi-insulating InP substrate and buried by a non-doped InP collector layer. The buried tungsten wires were fabricated only under the emitter mesa. There is no conductive layer under the extrinsic base region. Therefore, reduction of C_{BC} is achieved. We have fabricated the BM-HBT with emitter width of 2 μm by photolithography and confirmed remarkable reduction of total C_{BC} [4]. In the calculation result of RF characteristics, a marked increase in f_{MAX} is estimated when the emitter width is less than 0.5 μm, as shown in Fig. 1. Therefore, reduction of emitter size is significantly important to achieve high f_{MAX}.

In this letter, we describe the fabrication of InP/GaInAs based BM-HBT with submicron emitter. Electron beam lithography (EBL) was used for patterning completely through the process. In the SEM observation, the narrow emitter metal with good alignment of the buried tungsten wires was confirmed. DC and RF performances were measured and a current gain cutoff frequency (f_T) of 82 GHz and f_{MAX} of 200 GHz were obtained for the device with emitter width of 0.3 μm. Total C_{BC} was calculated from S-parameters and it was remarkably reduced in the BM-HBT.

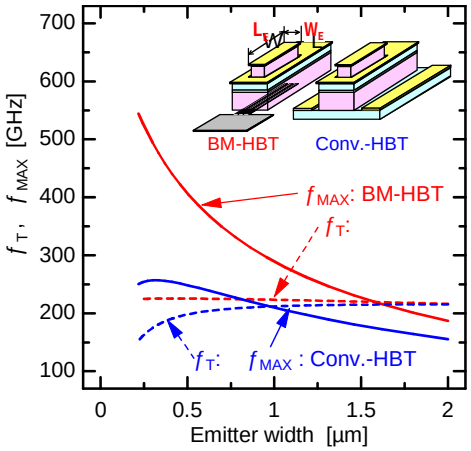

Fig.1. Calculated f_T and f_{MAX} of BM-HBT and conventional HBT on emitter width. When emitter width is reduced. BM-HBT provides higher f_{MAX}.

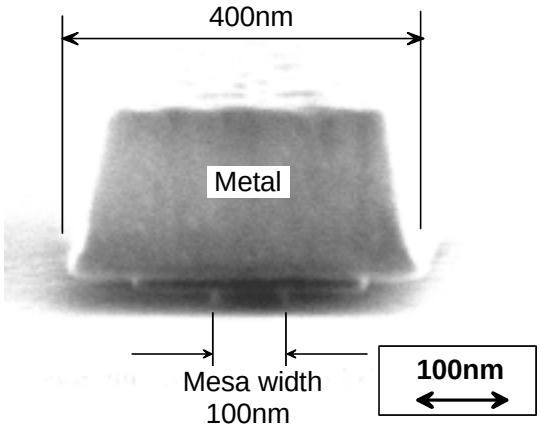

Fig. 2. Test structure of emitter. Mesa width was 100nm. Mesa was oriented along <010> direction.

Fabrication process of narrow emitter structure

To bury tungsten wires by an InP layer using organmetallic vapor phase epitaxy (OMVPE), the tungsten wires must be fabricated along <010> direction [5]. So, emitter finger of BM-HBT must be also fabricated along <010> direction. The emitter mesa, which is fabricated along this direction, has a (001) plane and a (010) plane at mesa side. Undercut etching of InP layer with (001) and (010) plane is not stopped, although undercut etching with (111)A or $(01\bar{1})$ plane is stopped, which are appeared plane at the side of the emitter mesa along $<01\bar{1}>$ or <011> direction [6]. By using this property, fine emitter mesa narrower than emitter electrode can be fabricated when the length of undercut etching is intentionally controlled.

To control the length of undercut etching, a slow and stable etching is required. So, solutions of etchant were kept at 3-5°C. Epitaxial structure with a 20-nm-thick GaInAs contact layer and a 30-nm-thick InP emitter layer was fabricated on a base layer. An emitter metal with 20-nm-thick Ti, 25-nm-thick Pt and 200-nm-thick Au was fabricated by liftoff technique using EBL. Poly-methyl-methacrylate (PMMA) was used as a resist. A GaInAs layer and an InP layer were etched by solutions of a citric acid:H_2O_2=5:1 and HCl:CH_3COOH=1:4, respectively. The length of undercut etching for the GaInAs layer was 50 nm when etching time was 90 sec, and the length of undercut etching for the InP layer was 100 nm when etching time was 30 sec. Total length of undercut etching restrained was 150 nm. The emitter structure with 100-nm-wide mesa could be formed when width of the emitter metal was 400 nm, as shown in Fig. 2.

To connect the emitter metal, opening process of contact holes on an insulation layer is essential. Diameter and separation of contact holes must be decreased with reduction of device size. In our previous report, opening process on benzocyclobutene layer using RIE was described, but transistor operation of conventional HBT with fine emitter narrower than 0.3 μm did not be confirmed [7]. Another method to connect the metal, airbridge, which enable to overlap interconnect metal to other metal without short instead of using insulation layer, is used. So, we fabricated an airbridge to make metal contact with the emitter. In actual fabrication, the dummy mesa of Au/Cr with the same thickness and lateral dimensions of emitter and base mesa was placed 2 μm from the base mesa. For the test structure of the airbridge, two dummy mesas were fabricated instead of the real and dummy mesas.

A double-layer resist with a 600-nm-thick PMMA layer and a 800-nm-thick ZEP520 layer was fabricated by spin coating. Top of the dummy emitter mesas were covered by a first-layered PMMA layer. Electron-beam exposure with dose of 250 μC/cm^2 was carried out just on the emitters for the legs of the airbridge and dose of 150 μC/cm^2 was used at the area between emitters for the bridge. By development with xylene, top of the emitters only were exposed and a PMMA layer between emitters was not removed. After evaporation of Au/Cr with 500nm/10nm in thickness and liftoff, airbridge structure was fabricated, as shown in fig. 3. The width of the leg of the airbridge was 300 nm. Accuracy of alignment in EBL was confirmed less than 50 nm. The legs can be aligned with a 400-nm-wide emitter electrode, which can form 100-nm-wide emitter mesa.

Fabrication of BM-HBT

We fabricated three types of devices with different dimensions. The areas of the emitter mesa were 0.3×1.5 μm^2, 0.5×2.5 μm^2 and 0.7×3.5 μm^2, the areas of the base mesa were 2.9×4.6μm^2, 3.1×5.6μm^2 and 3.3×6.6μm^2 and the numbers of buried tungsten wires were two, three and four, respectively.

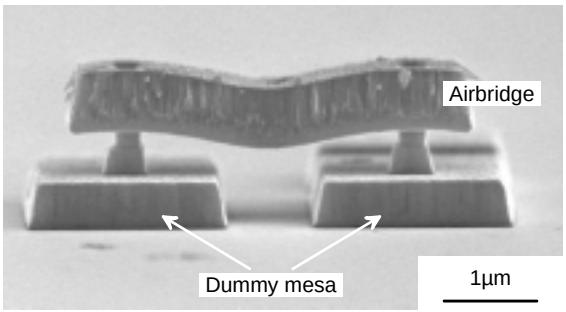

Fig. 3. SEM view of the test structure of the airbridge. The width of the leg and the thickness of the airbridge are 0.3 μm and 0.5 μm, respectively.

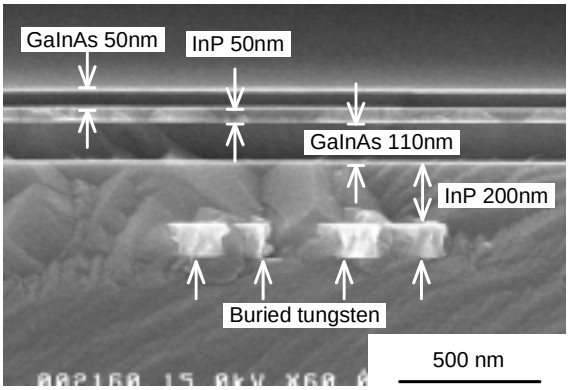

Fig. 4. Cross-sectional SEM view of buried tungsten wires. Four wires are observed. The thickness of the InP layer on the wires is 200 nm.

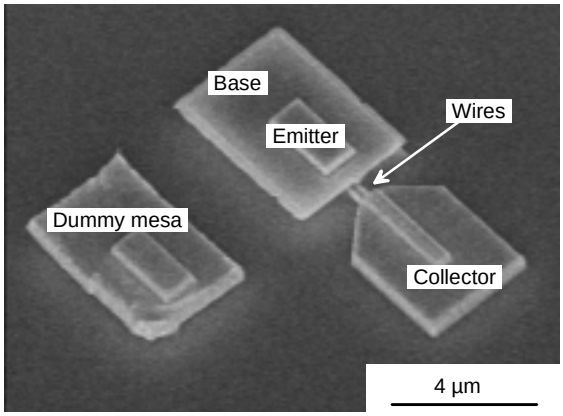

Fig. 5. SEM view of the fabricated BM-HBT with emitter width of 0.3 μm after formation of the dummy mesa. Good alignment between the wires and the emitter is observed.

The fabrication process is as follows. A 10-nm-thick GaInAs layer, a 100-nm-thick tungsten layer and a 20-nm-thick SiO_2 layer were fabricated on a (100) semi-insulating InP substrate. 20-nm-thick Cr stripes were fabricated by liftoff technique using EBL, which was used as an etching mask. The width and

period were 100 nm and 200 nm, respectively. At the same time, Cr masks for tungsten alignment marks ware fabricated. CF_4/O_2 reactive ion etching (RIE) fabricated fine tungsten wires by etching of SiO_2 and tungsten layers under a pressure of 3.8×10^{-3} Torr and a RF power of 20 W. Cr masks were removed by SiO_2 etching in a 7% buffered hydrofluoric acid. The exposed GaInAs layer, which is inserted between the semi-insulating substrate and tungsten film, was etched off to remove the damage by dry etching to the substrate. The inserted GaInAs layer remained just under the tungsten wires but did not affect transistor operation of the BM-HBT, because carriers were injected into the tungsten collector electrode from above.

Layer structures were fabricated using low-pressure OMVPE. Phosphine and arsine as group V materials, and trimethylindium and triethylgallium as group III materials were used. The tungsten wires were buried by InP growth with a thickness of 250 nm. Optimized growth conditions, growth temperature of 585°C, PH_3 flow rate of 500 sccm and InP growth rate of 42 nm/min, were used for the buried growth [5]. By successive growth, active layers of the HBT were fabricated with a 60-nm-thick i-GaInAs collector layer, a 50-nm-thick p-GaInAs base layer, a 50-nm-thick n-InP emitter layer and a 50-nm-thick n-GaInAs contact layer. To prevent diffusion of a p-type dopant, Zn, growth temperatures of the base layer and the emitter layer were lowered in 500°C and 530°C, respectively. Figure 4 shows the cross-sectional SEM view around four buried tungsten wires, which was the buried structure for the device with emitter width of 0.7 µm. A flat heterointerface was observed above the wires. The observed InP layer around the wires was thicker than that of a region without the wires. The thickness of the InP layer on the wires was measured to be 200 nm.

After the growth, an emitter mesa was fabricated by above-mentioned fabrication process with alignment to the buried tungsten wires using tungsten marks. The length of undercut etching was 300 nm. A base electrode of Ti/Pt/Au (20/25/20 nm in thickness) was fabricated by a self-alignment process. After protection of the emitter mesa by SAL601 resist, a base mesa was fabricated by a wet etching process and the device was isolated. At the same time, a part of the buried tungsten wires with 3-µm length were exposed for connection. A collector electrode of Ti/Au (10/500 nm in thickness) was fabricated on the exposed wires. Figure 5 shows the SEM view of the device with an emitter width of 0.3 µm after formation of the dummy mesa. Alignment between two buried wires and the emitter was confirmed from the position of the exposed wires. Wiring by airbridge between the emitter metal and the dummy emitter was fabricated by above-mentioned fabrication process. Finally, an interconnect pad metal was evaporated.

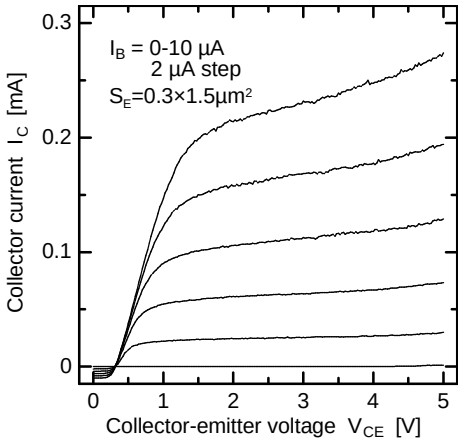

Fig. 6. Common-emitter collector I-V characteristics of the devices with an emitter area of 0.3×1.5 µm².

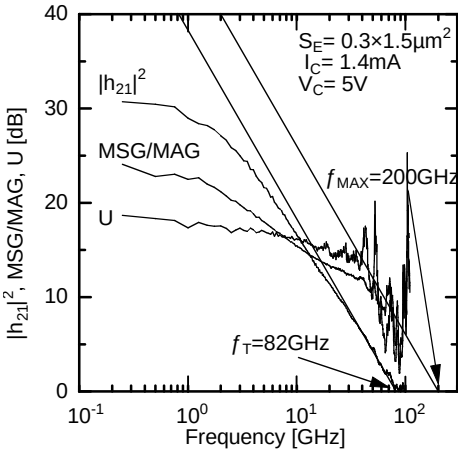

Fig. 7. Dependence of h_{21}, U and MSG/MAG in the range from 250 MHz to 110 GHz.

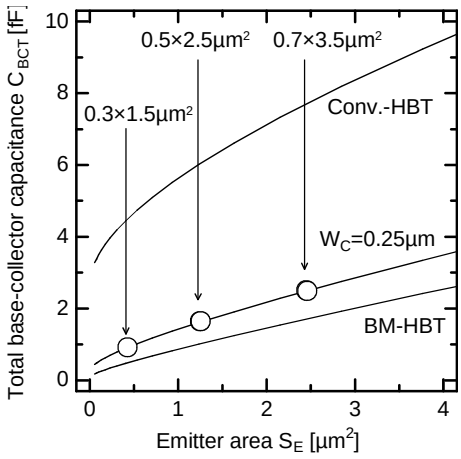

Fig. 8. : Total C_{BC} as a function of emitter area. Open circles denote measured C_{BC} for the devices with an emitter area of 0.3×1.5 µm², 0.5×2.5 µm² and 0.7×3.5 µm². Theoretical C_{BC} of BM-HBT and conventional HBT are calculated from physical dimensions. Broken line denotes C_{BC} when the conductive region under the base mesa is assumed to be the region around the wires with the width of 0.25 µm.

Result and discussion

Figure 6 shows common-emitter collector I-V characteristics of the device with emitter area of 0.3×1.5 μm^2. Current gain was about 20 at a collector current of 0.2 mA and a collector voltage of 3 V. Microwave S-parameters of the device were measured from 250 MHz to 110 GHz using network analyzer. Open and short characteristics of the interconnection pad were also measured, and the capacitance and the inductance were subtracted from the S-parameters of the devices. Figure 7 shows frequency dependences of current gain ($|h_{21}|^2$), Mason's unilateral gain (U) and maximum stable/available gain (MSG/MAG) at a collector current of 1.4 mA and a collector voltage of 5 V. f_T of 82 GHz was obtained from the –20 dB/decade extrapolation of $|h_{21}|^2$. On the other hand, U did not show the dependence of –20 dB/decade in the range over 40 GHz. So, we estimated f_{MAX} of 200 GHz from the value of U at 40 GHz.

Figure 8 shows total C_{BC} calculated from the imaginary part of Y_{12} parameters, which were 0.95 fF, 1.7 fF and 2.5 fF for the devices with emitter areas of 0.3×1.5 μm^2, 0.5×2.5 μm^2 and 0.7×3.5 μm^2, respectively. Theoretical C_{BC} of BM-HBT was calculated from physical dimensions of the devices and is shown by the solid lines with BM-HBT in Fig. 8. The difference of measured C_{BC} from theoretical C_{BC} of BM-HBT was less than 1 fF for three devices. Theoretical C_{BC} of conventional-HBT was also calculated with the same physical dimensions of a base mesa. Measured C_{BC} were 22-30% of calculated C_{BC} of conventional HBT. This result showed that C_{BC} was significantly reduced in the BM-HBT. To explain the difference between measured C_{BC} and theoretical C_{BC} of BM-HBT, we assumed that a conductive layer was generated at the grown interface around the tungsten wires. When the width of the conductive interface (W_C) of 0.25 μm was used as a fitting parameter, measured C_{BC} showed good agreement with the assumed C_{BC}, as shown in Fig. 8.

The measured capacitance of the interconnect pad was 4-5 fF and the difference of the measured C_{BC} and the theoretical C_{BC} was less than 1 fF. More precise measurement is also necessary to evaluate C_{BC}.

Conclusion

BM-HBTs with sub-micron emitter were fabricated by EBL process. The width of the smallest emitter in fabricated device was 0.3 μm. DC and RF performances were measured and f_T of 82 GHz and f_{MAX} of 200 GHz were obtained for the device with emitter width of 0.3 μm. Moreover, total C_{BC} of 0.95 fF was calculated from S-parameter measurement in the BM-HBT and was estimated to be about 22% of that of a conventional HBT calculated from the physical dimensions of the device. This result showed the possibility of high performance of BM-HBT.

Acknowledgement

The authors would like to thank Dr. Hara and Mr. Yamaura of Fujitsu laboratories for S-parameter measurement. The authors would like to thank Professor S. Arai, Professor M. Asada and Associate Professor M. Watanabe for their helpful discussions and encouragement. This work was supported by the Ministry of Education, Science, Sports and Culture through a Scientific Grant-In-Aid, the "Research for the Future" Program #JSPS-RFTF96P00101 from the Japan Society for the Promotion of Science (JSPS) and the Ministry of Public Management, Public Affairs, Posts and Telecommunications through the Grant for "Development of Frequency Resources".

References

[1] M. Sokolich, C. H. Fields and M. Madhav: IEEE Electron Device Lett. **22** (2001) 8.

[2] K. Kurishima, IEEE Trans. Electron Device, Vol. 43, No. 12, pp. 2074-2079, 1996.

[3] T. Arai, H. Tobita, Y. Harada, M. Suhara, Y. Miyamoto and K. Furuya: Proc. 11th Int. Conf. Indium Phosphide & Related Materials, Davos, Switzerland, 1999 (IEEE, Piscataway, 1999) p. 183.

[4] T. Arai, Y. Harada, S. Yamagami, Y. Miyamoto and K. Furuya: Jpn. J. Appl. Phys. **39** (2000) L503.

[5] T. Arai, H. Tobita, Y. Harada, M. Suhara, Y. Miyamoto and K. Furuya: Physica E, **7** (2000) 896.

[6]K. Kurishima, S Yamahata, H. Nakajima, H. Ito, and N. Watanabe: IEEE Electron Device Lett., **19** (1998) 303.

[7] T. Arai, S. Yamagami, Y. Okuda, Y. Harada, Y. Miyamoto and K. Furuya: submitted to IEICE Trans. Electron, vol.E84-C, no.10, oct., 2001.